

# Flexural Strengthening of Prestressed Girders with Partially Damaged Strands Using Enhancement of Carbon Fiber Laminates by End Sheet Anchorages

Hayder Qays Abbas  
Department of Civil Engineering  
University of Baghdad  
Baghdad Iraq  
haider\_q@yahoo.com

Alaa Hussein Al-Zuhairi  
Department of Civil Engineering  
University of Baghdad  
Baghdad Iraq  
alaalwn@coeng.uobaghdad.edu.iq

Received: 23 April 2022 | Revised: 13 May 2022 | Accepted: 21 May 2022

**Abstract-**This paper examines the impact of flexural strengthening on the percentage of damaged strands in internally unbonded tendons in partially prestressed concrete beams (0, 14.28%, and 28.57%) and the recovering conditions using CFRP composite longitudinal laminates at the soffit, and end anchorage U-wrap sheets to restore the original flexural capacity and mitigate the delamination of the soffit of longitudinal Carbon Fiber Reinforced Polymer (CFRP) laminates. The composition of the laminates and anchors affected the stress of the CFRP, the failure mode, and thus the behavior of the beam. The experimental results revealed that the usage of CFRP laminates has a considerable impact on strand strain, particularly when anchors are employed. The EB-CFRP laminates increased the flexural capacity by approximately 13%, which corresponds to strand damage of 14.28%, while flexural capacity increased by 9.3%, strand damage increased by 28.57% for members strengthened with laminates only, and around 21.58% and 16.85% for members reinforced with laminates and end anchorings. Quasi-experimental equations have been proposed to estimate the actual stress of untethered tendons considering the effect of CFRP laminates and final fixation winding.

**Keywords-**CFRP laminates; debonding; post-tensioned girder; strand damage; unbonded strand

## I. INTRODUCTION

Recent destructive failures of pre-stressed (PS) concrete bridges have prompted a reassessment of the condition of several PS members [1], giving rise to new postings and, in some cases, emergency closure. Some of these failures are the result of terrorist attacks involving explosives [2], which damage PS bridge members or tendons [3]. The losing strands on the concrete member have a great effect on the design PS force which reflects a reduction of the nominal capacity and lack of serviceability [4]. One of the strengthening findings that will be investigated in this paper is the evaluation of the use of CFRP laminates with and without end anchorages for strengthening enhancement. CFRPs are increasingly being used to strengthen and repair Reinforced Concrete (RC) structures. The advantages of using Fiber-Reinforced Polymer (FRP)

include the application's ease to use, the high ultimate strength, and corrosion resistance. The experimental results show that due to premature CFRP debonding from the concrete substrate, the maximum capacity of PS externally reinforced beams with CFRP sheets is not always completely realized. External FRP composites have emerged as a viable alternative to strengthening methods. FRP composites have been used for PS girder structures. It is not easy to determine strain and stress in unbonded tendons at ultimate flexural capacity due to the tendons' slip relatively to the surrounding concrete [5]. In practice, it is preferable to prevent the brittle failure mode by either eliminating it or shifting it to a more ductile mode. Anchoring the laminates to the concrete substrate with metallic or CFRP anchors may be a practical way to accomplish this [4]. CFRP U-wrapped anchors or other mechanical anchor systems have demonstrated high effectiveness in delaying the delamination process and increasing the strengthening efficiency. This study, along with [15], is a part of the ongoing investigating research regarding the efficiency of strengthening techniques that are conducted at Baghdad University (Civil Engineering Lab). The current paper focuses on the strengthening techniques using Externally Bonded CFRPs.

## II. MATERIAL PROPERTIES AND METHODOLOGY

### A. Design of the Tested Member

All tests were conducted in the laboratory of the College Faculty of Baghdad University under 4 points of loading as shown in Figures 1 and 4. Seven girders, as illustrated in Table II, have been used in this paper, spanning 3000mm and resting on simply supported ends of 2800mm apart. The specimens were reinforced with 2 $\phi$ 16mm at the bottom and 2 $\phi$ 10mm at the top whereas  $\phi$ 10mm bars were used for stirrups. Two unbonded strands were used inside the 22.5mm PVC duct with end grips, and the strand extended by 0.45m from each side. CFRP laminates ( $b_f=50$ mm and  $t_f=1.2$ mm) were attached to the soffit to strengthen the specimen in addition to two CFRP sheets at the end for anchorage purposes with  $t_f=0.167$ mm, set up on U wrapping shape as shown in Figure 2.

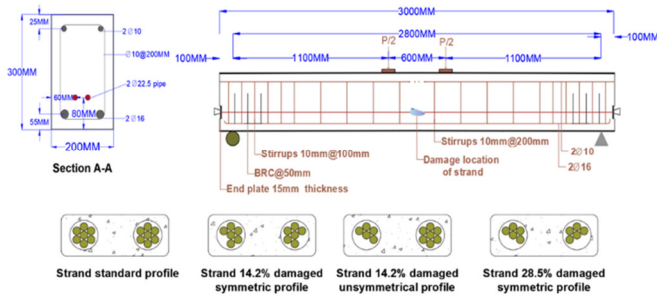


Fig. 1. Specimen and strand damage details.

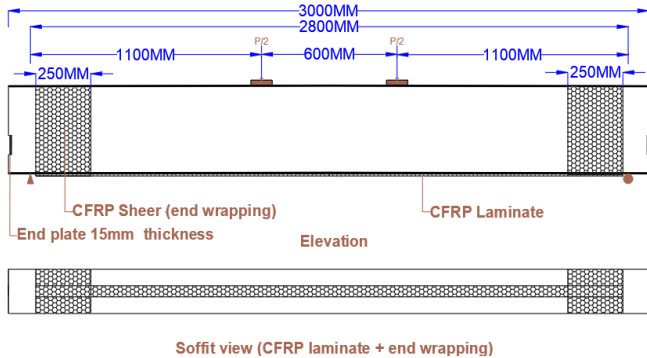


Fig. 2. Strengthening types considered in this study.

**B. Properties of the Tested Beams**

The design of the concrete mixture consisted of: Portland cement C45 with densities of 412kg/m<sup>3</sup> for cement, 1030kg/m<sup>3</sup> for aggregates, 548kg/m<sup>3</sup> for coarse sand, and 245kg/m<sup>3</sup> for fine sand (*f<sub>c</sub>*=44.60N/mm<sup>2</sup> and *f<sub>t</sub>*=5.80N/mm<sup>2</sup>), while 5.46lt/m<sup>3</sup> of superplasticizer were used. The yield, ultimate, strain, and area of steel bars are 518.20N/mm<sup>2</sup>, 658.970N/mm<sup>2</sup>, 12.20%, and 77.21mm<sup>2</sup> respectively for D10 bars and 577.30N/mm<sup>2</sup>, 710.74N/mm<sup>2</sup>, 13.40%, and 199.10mm<sup>2</sup> for D16 bars (*E<sub>s</sub>*=200000MN/m<sup>2</sup>). Nominal area, ultimate strength, yield strength, and ultimate strain were 98.7mm<sup>2</sup>, 1860.00MN/m<sup>2</sup>, 1725.00MN/m<sup>2</sup>, and 5.00% respectively for the 7 wires of Grade 270 unbonded tendons (*E<sub>s</sub>*=197.5GPa). The manufacturer provided the carbon fiber fabrics' mechanical properties in addition to the resin, in which the nominal thickness, tensile strength, and ultimate elongation were 1.2mm, 3100MN/m<sup>2</sup>, and 0.02 respectively for laminates (*E<sub>f</sub>*=170GPa), and 0.167mm, 3500MN/m<sup>2</sup>, 1.59% for unidirectional sheets (*E<sub>f</sub>*=220GPa).

The first letter B in the specimens' designation in Table II stands for beam, and the numbers 1 and 2 after the second letter designate the 14.25% and 28.57% strands damage groups, respectively. The letter R corresponds to individual group references, S to CFRP laminate strengthening, and W to laminate and end anchorage wrapping strengthening.

TABLE I. PROPERTIES AND LOCATIONS OF STRAIN GAUGES

Usage	Type	Ω	Adhesive type	QTY, location
Steel	FLAB-6-11	118.5±0.5	CN	2 @ tension bars
Strand	YEFLAB-2-3	119.5±0.5	CN	3
Concrete	PL-60-11	120±0.5	CN-E	2 @ 5cm below the top
CFRP	BFLAB-5-3	119.5±0.5	CN	2

**C. Recording Gauges and Setup**

All members were tested using a unidirectional electrical resistance strain gauge attached at the middle span to measure strain in the strand, FRP, concrete, and steel (Table I).

**D. Experimental Testing**

The steel cages were instrumented with strain gages of electric type before being placed in wood forms for concrete casting, using ready-mixed concrete. In addition to the dial gauge for measuring camber, the strain gauge wires were linked to a data logger to capture the strain of the strands during the pre-stressing process, as shown in Figure 3.



Fig. 3. Post-tensioning process.



Fig. 4. Test setup.

TABLE II. TESTED GIRDER DETAILS

Group	Girder ID	D (%)	Aps (mm <sup>2</sup> )	Laminate ( <i>L<sub>f</sub></i> )			Sheets ( <i>S<sub>f</sub></i> )			<i>ρ<sub>p</sub></i>	<i>ρ<sub>s</sub></i>	
				<i>t<sub>lf</sub></i>	<i>b<sub>lf</sub></i>	<i>L<sub>lf</sub></i>	<i>t<sub>sf</sub></i>	<i>b<sub>sf</sub></i>	<i>L<sub>sf</sub></i>			
				(mm)						(%)		
Ref.	B0	0	197.40	-	-	-	-	-	-	-	0.490	0.810
B1	B1R	14.28	169.20	-	-	-	-	-	-	-	0.385	
	B1S			1.2	50	2.7	-	-	-			
	B1SW			1.2	50	2.7	0.167	250	76			
B2	B2R	28.57	141.00	-	-	-	-	-	-	-	0.320	
	B2S			1.2	50	2.7	-	-	-			
	B2SW			1.2	50	2.7	0.167	250	76			

Two 1cm thick end steel plates were used at the ends of each specimen with the incision at one of the endplates to protect and guide the strain gauge's wires during the pre-stressing process. The 2 endplates were punched with 2.2cm diameter PS ducting. For anchorage at the unbonded strands, 2 pieces of split-wedge anchor grips (barrel-type) were used. The grips were attached to the ends of the strands, which were then marked using a permanent marker to determine the pre-strain level that was applied in each strand. ( $\Delta L=15.5$ cm as per the member design required). The first strand was pulled out to the requisite pre-stressing value in two stages: initial for starching the strand and final to the preferred pre-stressing value. Then the piston was released. The procedure was then repeated with the second strand, with pressure gauge readings from the hydraulic jack used in the post-tensioning procedure [6]. Two

dial gauges were attached to each end of the strand to find out the slipping of the strand slip during the loading process. Four LVDTs were used to measure the deflection of the 2 specimens near the support, one under the point load, and the other under the quarter point. All LVDTs were set up to zero strain at the start of testing as shown in Figure 4. To progressively raise the load, a 50-ton hydraulic jack was installed to a load cell with a maximum capacity of 50ton. Increments of 15kN were added until the cracking load was reached. The load was then applied in 30kN increments until failure occurred. Each beam took approximately 2 to 3 hours to complete the test. The load cell was used to monitor the applied load from the frame of the test and to collect the reading data. The applied cracks were signified for each load step after the appearance of the first crack. The fracture pattern on the 2 sides of the cross-section was captured on camera after the test. The modes and ultimate loads of failure were reported. During testing, the first crack and crack propagation were monitored as well as the load deflection.

### III. RESULTS

The test girders' performance was measured in terms of maximum load-bearing capability. All the reference girders failed in the compression zone due to flexure tensile steel reinforcing yielding, whereas the strengthened beams failed by laminate debonding followed by sudden compression and tension of concrete and steel bars (Figure 6). The first flexural crack appeared in the midspan of sub-reference girders PC1R, and PC2R, with respective cracking loads approximately 94%, and 85% of the reference girder's cracking load. The cracking propagation is typically shown in Figure 5 at the end of the test members in the various test series.

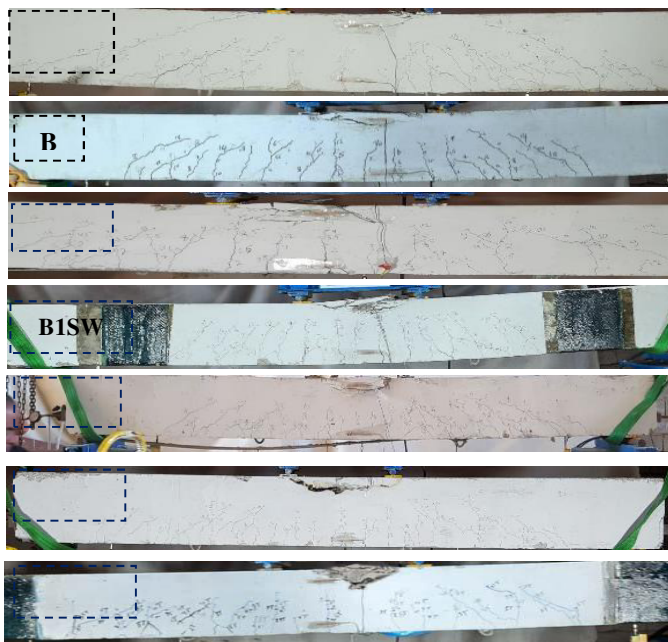


Fig. 5. Representative beam crack patterns.

When the specimens were subjected to the externally applied load, the cracking patterns were quite similar and

typical of flexural members. During the initial cyclic loading between  $P_{min}$  and  $P_{max}$ , the first flexural cracks appeared within the constant moment zone. Table III shows the cracking loads  $P_{cr}$  for the various members before FRP application. As the applied load increased, the number of cracks increased as they began to form within the shear zone. The cracks tended to separate as the load increased and additional flexural cracks were formed. Table III contains a summary of the members' modes of failure. Unbonded PC specimens failed due to concrete crushing, CFRP ultimate strain (rupture), CFRP debonding, or combinations of these modes. The propagation of interface cracks in the concrete near the CFRP in a horizontal direction along with the embedded tension reinforcement until connecting with the vertical flexural cracks caused peeling off of the concrete cover, indicating FRP debonding failure. The control girder failed in a more brittle mode than the strengthened girders, which was evidenced by faster crack propagation and fewer cracks but with wider widths, whereas the control girder showed a more brittle mode [7]. That is explained by the propagation of fewer and faster cracks in wide widths. A large number of cracks with smaller widths occurred for girders strengthened by carbon fibers.



Fig. 6. Representative beam failure modes.

#### A. Flexural Capacity and Load Deflection

The tested members were investigated at 3 different load levels: cracking loads, post cracking elastic stage, and peak loads as shown in Figure 7. The CFRP laminates and tendons had almost no influence on the member behavior when the applied load did not reach the cracking load. The findings demonstrate that Group 1 and 2 exhibited more strength than the undamaged member. However, the strengthened members with laminates exhibited an increase in flexural capacity of 13-9% for groups 1 and 2 and 21-16% for laminates with anchors when compared to the undamaged girders of the same group as illustrated in Figure 7, indicating the effect of the end anchorage on strength and ductility. The stiffness of the reference girders decreases slightly and the strengthened girders did not significantly differ from the damaged reference girders of the same group. When the applied load exceeded the cracking load, the damaged members exhibited a relatively high rate of stiffness deterioration [8] due to the absence of a portion of the pre-stressing force, which increases the development rate of crack and displacement. Likewise, the flexural-strengthening CFRP EB of the laminates exhibited their ability to postpone the fracture formation and deterioration of the stiffness of the strengthened girders [9], and the girders strengthened with laminates and anchors were observed to be superior to the girders strengthened with laminates only. The deflection is at the same value as the applied load which is equal to 0.79 of the ultimate load. The serviceability limitation for deflection (span over 250) is considered and the corresponding value is used in this paper, as

per the result of control, the deflection at the serviceability limit is 1.12cm and this value is referred to as the permissible load which is about 79% of the ultimate load. The displacement of the strengthened girders was slightly reduced by 9–18% for B1S and B2S whereas almost the same amount (11-19%) of reduction occurred for B1SW and B2SW. It should be noted that in each case, the member with the end anchorage had a smaller drop in the value of the load, higher strength, and much more stiffness [10]. The CFRP girders strengthened with CFRP laminates and U-wrapping of CFRP sheets demonstrated

increased deflection at the maximum load due to the absence of a relatively gradually load drop after the initiation of partial debonding. The ability of the members with an anchor to preserve their ductile response was exhibited. The ultimate displacement increased significantly when the specimen strengthened with laminates only and laminates with end anchorage, and the increment reached 18.16% and 11.39% respectively for B1SW and B2SW in comparison with B1S and B2S.

TABLE III. SUMMARY OF SPECIMEN TESTING AND RESULTS

Girder ID	Cracking load (kN)	Cracking load concerning control (%)	Ultimate load (kN)	Mid-span deflection at ultimate load (mm)	$P_{cr}/P_{ult}$ (%)	Change in flexural strength (%)		Failure mode
B0-control	55.03	-	166.240	26.9	33.10	-		SF, CC
B1R	52.05	94.5	157.250	25.5	33.10	5.410	R	SF, CC
B1S	62.79	14.06	187.990	24.1	33.40	13.080	I	SF, CC-DL
B1SW	66.78	25.9	202.120	28.5	33.00	21.580	I	SF, CC-CD
B2R	47.00	85.38	148.710	29.9	31.60	10.540	R	SF, CC
B2S	58.37	6.09	182.420	23.8	32.00	9.730	I	SF, CC-DL
B2SW	62.16	21.21	194.250	26.5	32.00	16.850	I	SF, CC-CD

SF, steel failure at tension zone, CC crushing of concrete, DL, delamination of CFRP laminate. CD covers delamination, a Negative sign is for reduction, and a positive sign is for increasing. R is for reduction, and I is for increase

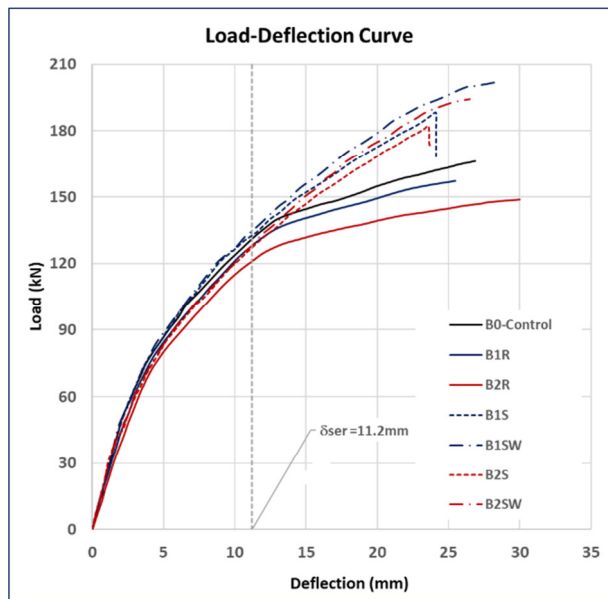


Fig. 7. Load deflection curves.

### B. Applied Load and Strain for the CFRP Laminates

The cracks in CFRP laminates before the cracking load are minimal and nearly equal (Figure 6). After the load reaches the cracking load, the strain clearly increases, and after the bonded steel reinforcement yields, the strain increment rate increases significantly. The increased rates of strain in the CFRP laminates, with and without the end anchors, were almost similar but the maximum strain of the strain increases in CFRP laminates end by anchors was much higher. At the serviceability load limit, the rise in a strain of strengthened members B1S and B2S was 0.265% and 0.346%, in comparison with the 13.25% and 17.3% of the ultimate strain of laminate capacity ( $\epsilon_{fju} = 2\%$ ) with no significant change to the strengthened specimens with laminates and anchorage sheets, B1SW and B2SW. The strain increase at the ultimate

load was 0.830% and 0.90% corresponding to 41.5% and 45.1% of the ultimate strain of the fiber capacity of B1S and B2S. The B1SW and B2SW specimens achieved more strain at the ultimate load, which is about 1.0235% and 1.033% corresponding to the 51% of the laminate strain capacity. Furthermore, the use of FRP laminates with end U-wrapping anchorage sheets had a significant impact on the compressive concrete strain. The CFRP laminates, as previously mentioned, were able to stop the development of cracks in their path.

### C. Applied Load and Effect on the Strands Strain

Because of the minor strain increases, the strand did not contribute to flexural strength before the first crack. The increase in the strand strain was calculated by subtracting the post-tensioning initial strain from the actual strain (Figure 8). During this loading stage, the strand exhibited the same behavior in all the tested members. The strain increases in the strand for the references groups 1 and 2 were greater than the control girder's, whereas the strand strain increases in the members strengthened with laminates was less than in the same group members without strengthening. At the serviceability load limits, the increase in the strand strain for B1R and B2R was  $7500\mu\epsilon$  and  $89501\mu\epsilon$ , representing an increase of 8.5% and 29.5% from the control member. Similarly, the strain increases in the strands of the strengthened girders B1S and B2S were  $6750\mu\epsilon$  and  $7620\mu\epsilon$ , with a reduction of 14.670% and 14.860%. The references' strand strain increments were much smaller in the loading stage after the load in the serviceability manner in the strengthened members B1S and B2S at the same loading level. The lessening of the tendon strain increases in the member strengthened with end anchors was 14.67% and 17.88% for B1SW and B2SW girders. The above results prove that the CFRP strengthened with laminates, including the end U-wrapped anchors, have a great influence on the behavior of the strands. As previously mentioned, the CFRP laminates were able to delay the cracks, prevent their development, and slow down the degradation of the member stiffness.

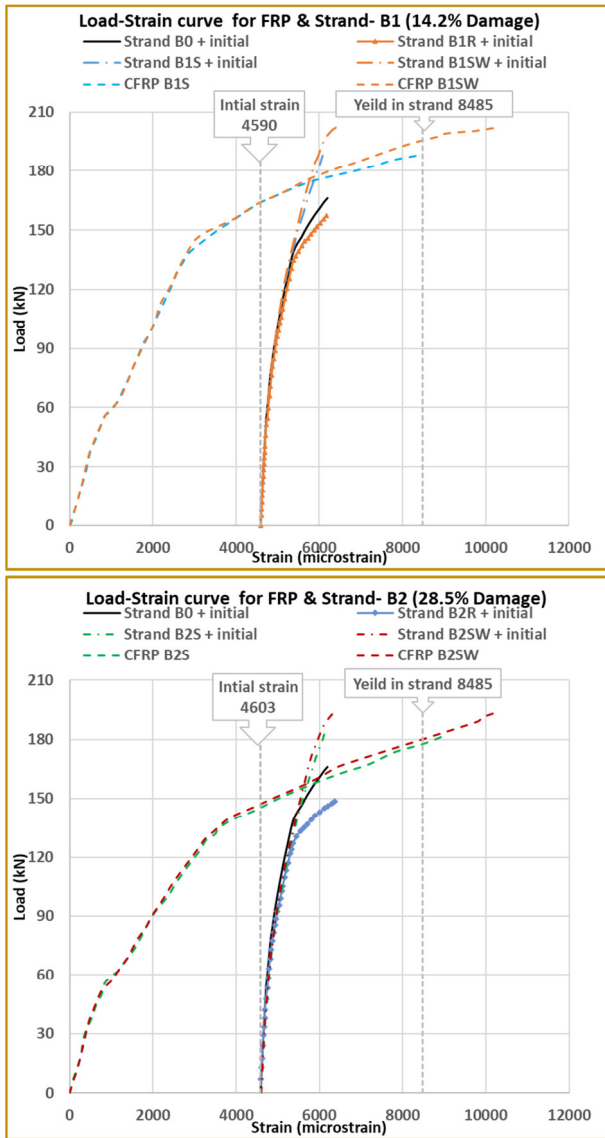


Fig. 8. CFRP and strands load-strain.

IV. EVALUATING THE NOMINAL MOMENT CAPACITY OF THE MEMBER

A. The Increased Strain in the Strands

Determining the increase in a strain of unbonded strands is a critical case in estimating the flexural strength of unbonded post-tension members strengthened with CFRP laminates. Regrettably, the design guidelines, such as [11] have only suggested one approach to evaluate the increase in the strain of bonded post-tendons and pre-tension members strengthened with EB-CFRP sheets, whereas the correlating approaches for unbonded strands in members strengthened with CFRP laminates were not included. Additionally, the result of the experimental work exhibited that CFRP laminates significantly influence the unbonded tendons' behavior [5]. The increase in the strain of the strand of the unbonded post-tension member strengthened with CFRP was evaluated using the equations for unbonded tendons in normal reinforced concrete members, as below [12]:

For members without end CFRP U-wrapped sheet anchors:

$$\Delta_{\epsilon_{ps,CFRP}} = \psi \epsilon_c \left( \frac{d_p - c}{L_0} \right) \times \left( 1 + 100 \frac{A_f E_f \epsilon_{fe}}{A_c E_c \epsilon_{fu}} \right)^{0.59} \quad (1)$$

For members with end CFRP U-wrapped sheet anchors:

$$\Delta_{\epsilon_{ps,CFRP}} = \psi \epsilon_c \left( \frac{d_p - c}{L_0} \right) \times \left( 1 + 100 \frac{A_f E_f \epsilon_{fe}}{A_c E_c \epsilon_{fu}} \right)^{1.35} \quad (2)$$

The overall strain of the unbonded strands  $\Delta_{\epsilon_{ps,CFRP}}$  is calculated as:

$$\epsilon_{ps,CFRP} = \epsilon_{pe} + \Delta_{\epsilon_{ps,CFRP}} \quad (3)$$

where  $\epsilon_{fe}$  is the initial strain of a strand not including strain losses =  $F_p / (E_p A_p)$ ,  $F_p$  (N) is the actual tensile force in a strand,  $A_p$  (mm<sup>2</sup>) and  $E_p$  (MPa) are the cross-sectional area and elasticity modulus of a strand respectively,  $\Delta_{\epsilon_{ps,CFRP}}$  is the increase in a strain of strands,  $\psi$  is "the length of the plastic zone divided by the height of the compressive concrete zone":  $\psi = 10.50$  [13] for un-cracked, simply supported unbonded post-tensioned members, reinforced with CFRP laminates, and  $\psi = 9.80$  [14] for pre-cracked unbonded post-tensioned members reinforced by EB-CFRP,  $\epsilon_c$  is the maximum strain at the concrete compression fiber [11],  $d_p$ , (mm) is the distance between the compressive concrete fiber's furthest point and the centroid of the strands' cross-sectional area,  $c$  (mm) represents the compression zone height [6],  $L_0$  (mm) represents the effective span of the member, and  $\epsilon_{fe}$  represents the actual strain in CFRP laminates at the ultimate applied load.

B. Evaluation of the Proposed Formula

The suggested equations (2)–(4) were applied for the estimation of flexural strength of the 23 unbonded post tensioned members reinforced with CFRP laminates including the 7 simply supported members reinforced with EB-CFRP laminates investigated in this manuscript and the 16 slabs and beams of [7]. The theoretical (predicted) flexural strength,  $M_{u,pred}$ , was calculated as per [11] considering 1.0 as the factor of strength reduction, as below:

- Step # 1: Estimation of the compression concrete zone depth.

The depth of the neutral axis,  $c$  (mm), is initially assumed as depth/10 [11].

- Step # 2: Evaluate the strain in CFRP laminates, concrete, and strands.

The CFRP laminate strain,  $\epsilon_{fe}$ , for failure detected by concrete crushing is:

$$\epsilon_{fe} = \epsilon_{cu} \left( \frac{d_f - c}{c} \right) - \epsilon_{bi} \leq \epsilon_{fd} \quad (4)$$

where  $d_f$  is the effective CFRP laminate depth,  $\epsilon_{cu}$  is the concrete's ultimate compressive strength which is equal to 0.003, and  $\epsilon_{bi}$  represents the initial strain in the substrate:

$$\epsilon_{bi} = \frac{-F_p}{E_c A_c} \left( 1 + \frac{e y_b}{r^2} \right) + \frac{M_{DL} y_b}{I_c A_c} \quad (5)$$

where  $F_p$  is the initial prestressing force (N) after excluding the losses,  $e$  (mm) represents the prestressing force's eccentricity

concerning the concrete cross-centroid section,  $y_b$  (mm) represents the distance from the gross-centroidal section (ignoring steel rebars) to the farthest bottom fiber,  $r$  (mm) represents the radius gyration of the member section  $= (I_c/A_c)^{0.5}$ ,  $I_c$  (mm<sup>4</sup>) represents the moment of inertia of concrete cross concerning the neutral axis,  $M_{DL}$  (N.mm) is the applied dead load's moment, and  $\epsilon_{fd}$  is the strain's debonding, defined by:

$$\epsilon_{fd} = 0.41 * \sqrt{\frac{f'_c}{nE_c t_f}} \leq 0.9\epsilon_{ffu} \quad (6)$$

where  $f'_c$  is the concrete strength,  $\epsilon_{ffu}$ ,  $t_f$ , and  $E_f$  are the ultimate strain, thickness, and elasticity modulus of CFRP respectively, and  $n$  represents the CFRP layer's numbers.

The strain in CFRP laminate,  $\epsilon_{fe}$ , for failure detected by the rupture of prestressing strands is:

$$\epsilon_{fe} = (\epsilon_{pu} - \epsilon_{pi}) \left( \frac{d_f - c}{c} \right) - \epsilon_{bi} \leq \epsilon_{fd} \quad (7)$$

where  $\epsilon_{pu}$  is the strand rupture strain which is equal to 0.05 and  $\epsilon_{pi}$  is the strand initial strain, which can be estimated as:

$$\epsilon_{pi} = \frac{F_p}{E_c A_c} + \frac{F_p}{E_c A_c} \left( 1 + \frac{e^2}{r^2} \right) \quad (8)$$

- Step # 3: Estimation of the steel rebars strain,  $\epsilon_s$ :

$$\epsilon_s = (\epsilon_{fe} + \epsilon_{pi}) \left( \frac{d - c}{d_f - c} \right) \quad (9)$$

- Step # 4: The depth of  $c$  must be recalculated, using the summation of forces equal to zero.

$$c = \frac{A_p f_{ps} + A_s f_s + A_f f_{fe}}{\alpha_1 f'_c \beta_1 b} \quad (10)$$

where  $f_{fe}$  (MPa) is the CFRP laminate stress  $= E_f \times \epsilon_{fe}$ ,  $f_{ps}$  (MPa) is the strand's stress  $= E_p \times \epsilon_{ps,CFRP} \leq f_{py}$ , and  $f_s$  (MPa) is the tensile rebars' stress  $= E_s \times \epsilon_s \leq f_y$ .

- Step # 5: Checking the  $c$  for the depth of the compressive concrete zone.

Now, when the assumed value of  $c$  ( $c_{assumed}$ ) and the calculated through the above equations ( $c_{calculated}$ ) meet the presented criterion of convergence in (11), the appropriate value of  $c$  is obtained. If not, another  $c_{assumed}$  value is calculated, and the process is iterated starting at the second step until convergence is achieved.

$$\text{criterion of convergence} = \frac{|c_{assu} - c_{cal}|}{c_{assu}} \leq 0.1\% \quad (11)$$

- Step # 6: Evaluating the flexural strength of EB-CFRP strengthened member.

The flexural strength of the EB-CFRP strengthened unbonded prestressed concrete member,  $M_{u, pred}$  can be calculated as:

$$M_{u, pred} = A_p f_{ps} \left( d_p - \frac{\beta_1 c}{2} \right) + A_f f_{fe} \left( d_f - \frac{\beta_1 c}{2} \right) + A_s f_s \left( d - \frac{\beta_1 c}{2} \right) + A'_s f'_s \left( \frac{\beta_1 c}{2} - d' \right) \quad (12)$$

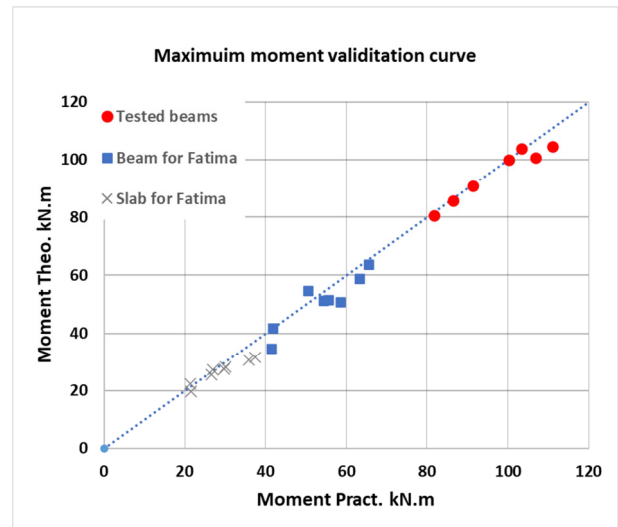


Fig. 9. Flexural capacity predictions and experimental results comparison.

TABLE IV. THEORETICAL AND PREDICTED VALUE COMPARISON

Members from [7]				Members from this study			
Member	$M_{u-P}$	$M_{u-E}$	$M_{u-P}/M_{u-E}$	Member	$M_{u-P}$	$M_{u-E}$	$M_{u-P}/M_{u-E}$
UB1_H_F1	41.778	41.800	0.999	B0	90.706	91.43	0.99
UB1_H_F2	51.381	54.300	0.946	B1R	85.734	86.49	0.99
UB1_P_F1	34.749	41.400	0.839	B1S	103.774	103.39	1.00
UB1_P_F2	51.678	55.600	0.929	B1SW	104.61	111.17	0.94
UB2_H_F1	54.846	50.500	1.086	B2R	80.498	81.80	0.984
UB2_H_F2	63.855	65.500	0.975	B2S	100.0175	100.33	1.00
UB2_P_F1	50.787	58.500	0.868	B2SW	100.7985	106.84	0.94
UB2_P_F2	58.905	63.300	0.931	Average M			0.979
US1_H_F1	22.374	21.400	1.046	Standard deviation SD			0.026
US1_H_F2	27.324	26.900	1.016	COV			2.63%
US1_P_F1	19.701	21.600	0.912	<b>Totals</b> <b>M</b> 0.953 <b>SD</b> 0.063 <b>COV</b> 6.56% $M_{u-P}$ is the theoretical (predicted) and $M_{u-E}$ is the experimental value			
US1/P/F2	28.314	30.100	0.941				
US2_H_F1	25.443	26.600	0.957				
US2_H_F2	30.690	35.800	0.857				
US2_P_F1	27.423	29.800	0.920				
US2_P_F2	31.680	37.400	0.847				
Average M			0.942				
SD			0.071				
COV			7.5%				

The predicted-to-experimental flexural strength ratios are illustrated in Table IV and Figure 9. The mean value of 0.953 and the Coefficient of Variation (COV) of 6.56%, describe the precision of the theoretical flexural strength values and their applicability for predicting the flexural strength of the EB-CFRP reinforced unbonded prestressed concrete members with and without wrapped sheet anchorages.

## V. CONCLUSION

- Beams outfitted with the proposed U-anchor had an about 15% higher debonding load, as well as companion beams with the anchor have a higher maximum load and corresponding deflection. Anchors experienced greater CFRP strain than their counterpart members without anchorages, and the maximum strain is much more than the theoretical strain-based [11] The anchorage was discovered to be effective in restricting the extent of debonding of the laminate, thus indirectly contributing to member flexural stiffness by restricting the crack width.
- For the same loading level, the flexural capacity of post-tensioned girders decreases as the strand damage ratio increases, whereas the displacement of girders increases the damaged strands ratio. The test results exhibited flexure capacity losses up to 5.4% for B1R and 10.54% for B2R at midspan for damaged strands, and for a strengthened member the flexural capacity gained back the lost strength due to the strand's damage and increased it by (13.08%, 26.47%, for B1S and B1SW, whereas for B2S and B2SW the enhancement was 9.73% and 25.25% respectively).
- Prestressed concrete element members with more than 20% damaged strands must meet the serviceability requirements before using enhancing procedures.
- The proposed equations for tendon strain in unbonded prestressed reinforced concrete members reinforced with EB-CFRP laminates, provide flexural capacity predictions with high precision and minimal variation with a mean equal to 0.95 and COV equal to 0.067.

## REFERENCES

- [1] A. M. Al-Hilali, A. F. Izzet, and N. Oukaili, "Static Shear Strength of a Non-Prismatic Beam with Transverse Openings," *Engineering, Technology & Applied Science Research*, vol. 12, no. 2, pp. 8349–8353, Apr. 2022, <https://doi.org/10.48084/etasr.4789>.
- [2] B. F. Abdulkareem, A. F. Izzet, and N. Oukaili, "Post-Fire Behavior of Non-Prismatic Beams with Multiple Rectangular Openings Monotonically Loaded," *Engineering, Technology & Applied Science Research*, vol. 11, no. 6, pp. 7763–7769, Dec. 2021, <https://doi.org/10.48084/etasr.4488>.
- [3] H. M. Hekmet and A. F. Izzet, "Performance of Segmental Post-Tensioned Concrete Beams Exposed to High Fire Temperature," *Engineering, Technology & Applied Science Research*, vol. 9, no. 4, pp. 4440–4447, Aug. 2019, <https://doi.org/10.48084/etasr.2864>.
- [4] G. Razaqpur and A. B. Mostafa, "C-Anchor for Strengthening the Connection between Adhesively Bonded Laminates and Concrete Substrates," *Technologies*, vol. 3, no. 4, pp. 238–258, Dec. 2015, <https://doi.org/10.3390/technologies3040238>.
- [5] L. Nguyen-Minh *et al.*, "Flexural-strengthening efficiency of cfrp sheets for unbonded post-tensioned concrete T-beams," *Engineering Structures*, vol. 166, pp. 1–15, Jul. 2018, <https://doi.org/10.1016/j.engstruct.2018.03.065>.
- [6] ACI Committee 318, *ACI CODE-318-19: Building Code Requirements for Structural Concrete and Commentary*. Farmington Hills, MI, USA: ACI, 2019.
- [7] F. El Meski and M. Harajli, "Flexural Behavior of Unbonded Posttensioned Concrete Members Strengthened Using External FRP Composites," *Journal of Composites for Construction*, vol. 17, no. 2, pp. 197–207, Apr. 2013, [https://doi.org/10.1061/\(ASCE\)CC.1943-5614.0000330](https://doi.org/10.1061/(ASCE)CC.1943-5614.0000330).
- [8] A. A. Abdulhameed *et al.*, "The Behavior of Hybrid Fiber-Reinforced Concrete Elements: A New Stress-Strain Model Using an Evolutionary Approach," *Applied Sciences*, vol. 12, no. 4, Jan. 2022, Apr. No. 2245, <https://doi.org/10.3390/app12042245>.
- [9] A. H. Al-Zuhairi, A. H. Al-Ahmed, A. A. Abdulhameed, and A. N. Hanoon, "Calibration of a New Concrete Damage Plasticity Theoretical Model Based on Experimental Parameters," *Civil Engineering Journal*, vol. 8, no. 2, pp. 225–237, Feb. 2022, <https://doi.org/10.28991/CEJ-2022-08-02-03>.
- [10] A. H. Al-Zuhairi and A. I. Taj, "Effectiveness of Meso-Scale Approach in Modeling of Plain Concrete Beam," *Journal of Engineering*, vol. 24, no. 8, pp. 71–80, Jul. 2018, <https://doi.org/10.31026/j.eng.2018.08.06>.
- [11] ACI Committee 440, *ACI PRC-440.2-17: Guide for the Design and Construction of Externally Bonded FRP Systems for Strengthening Concrete Structures*. Farmington Hills, MI, USA: ACI, 2017.
- [12] A. Tam and F. N. Pannell, "The ultimate moment of resistance of unbonded partially prestressed reinforced concrete beams," *Magazine of Concrete Research*, vol. 28, no. 97, pp. 203–208, Dec. 1976, <https://doi.org/10.1680/mac.1976.28.97.203>.
- [13] F. T. K. Au and J. S. Du, "Prediction of ultimate stress in unbonded prestressed tendons," *Magazine of Concrete Research*, vol. 56, no. 1, pp. 1–11, Feb. 2004, <https://doi.org/10.1680/mac.2004.56.1.1>.
- [14] F. El Meski and M. Harajli, "Evaluation of the Flexural Response of CFRP-Strengthened Unbonded Posttensioned Members," *Journal of Composites for Construction*, vol. 19, no. 3, Jun. 2015, Art. no. 04014052, [https://doi.org/10.1061/\(ASCE\)CC.1943-5614.0000516](https://doi.org/10.1061/(ASCE)CC.1943-5614.0000516).
- [15] A. J. Daraj and A. H. Al-Zuhairi, "The Combined Strengthening Effect of CFRP Wrapping and NSM CFRP Laminates on the Flexural Behavior of Post-Tensioning Concrete Girders Subjected to Partially Strand Damage," *Engineering, Technology & Applied Science Research*, vol. 12, no. 4, pp. 8856–8863, Aug. 2022, <https://doi.org/10.48084/etasr.5008>.